Journal of Fluorescence (2022) 32:1143–1154
https://doi.org/10.1007/s10895-022-02922-5

ORIGINAL ARTICLE

Dual Fluorometric Detection of Fe^{3+} and Hg^{2+} Ions in an Aqueous Medium Using Carbon Quantum Dots as a "Turn-off" Fluorescence Sensor

Shafali Singh[1] · **Sushil Kumar Kansal**[1]

Received: 25 November 2021 / Accepted: 1 March 2022 / Published online: 23 March 2022

Abstract
The present study aimed to develop a carbon dots-based fluorescence (FL) sensor that can detect more than one pollutant simultaneously in the same aqueous solution. The carbon dots-based FL sensor has been prepared by employing a facile hydrothermal method using citric acid and ethylenediamine as precursors. The as-synthesized CDs displayed excellent hydrophilicity, good photostability and blue fluorescence under UV light. They have been used as an efficient "turn-off" FL sensor for dual sensing of Fe^{3+} and Hg^{2+} ions in an aqueous medium with high sensitivity and selectivity through a static quenching mechanism. The lowest limit of detection (LOD) for Fe^{3+} and Hg^{2+} ions was found to be 0.406 μM and 0.934 μM, respectively over the concentration range of 0-50 μM. Therefore, the present work provides an effective strategy to monitor the concentration of Fe^{3+} and Hg^{2+} ions simultaneously in an aqueous medium using environment-friendly CDs.

Keywords Carbon dots · Fluorescence · Heavy metals · Dual sensing · Static quenching · Detection limit

Introduction

Efficacious monitoring and surveillance of water quality have become a paramount task, globally in the twenty-first century. Though it is, by far, the most essential resource for the existence of life on earth, a large number of people across the world are suffering from a lack of access to clean and safe drinking water. According to a report by World Water Council, it is expected that the number of people living in areas with water scarcity will likely reach a figure of 3.9 billion by the year 2030. As a result of this lack of access, these people, often belonging to poor developing countries are forced to consume water that is unsafe for drinking purpose, thereby resulting in large numbers of deaths every year. According to a report of the United Nations, approximately 1.7 million people die every year due to the forced consumption of unsafe drinking water [1, 2]. The major reason behind this decline in water quality is the discharge of wastewater containing toxic substances from farms, households, and industries into the freshwater streams. These toxic substances or pollutants could be anything—fertilizers, municipal waste, industrial waste, pesticides, or even waste leaching from landfills and leaking septic systems [3–6]. Among these pollutants, heavy metals have a significant contribution to the retrogression of water quality due to their adverse effects on the ecosystem [7, 8]. The outbreak of heavy metal poisoning brings an evolution from single metal pollution in the twentieth century to mixed metal pollution in the twenty-first century. A majority of heavy metals have been detected at concentrations much higher than the threshold limits of WHO and USEPA standards. They get leached from the soil to the groundwater via surface water leading to adverse health effects in all kinds of living organisms. Since they cannot be degraded, they end up getting accumulated in plants, animals, and food chains in high concentrations [9, 10]. Among the various heavy metals, Fe^{3+} ion plays a vital role in various biological activities in the human body including oxygen transport, enzyme catalysis, DNA synthesis, electron transport, the formation of free radicals, a cofactor in enzyme-based reactions, and cellular metabolism. The deficiency of Fe^{3+} ion can cause many diseases such as heart failure, anemia, tissue damage, Parkinson's disease, kidney and liver damage, Alzheimer's disease, cancer, arthritis, and diabetes. But beyond a certain threshold

✉ Sushil Kumar Kansal
sushilkk1@yahoo.co.in; sushilkk1@pu.ac.in

[1] Dr. S. S. Bhatnagar University Institute of Chemical Engineering and Technology, Panjab University, Chandigarh 160014, India

limit, Fe^{3+} ion becomes toxic and can cause harmful effects in the human body [11–13]. Additionally, Hg^{2+} ion detection is gaining utmost attention due to its high toxicity, great water solubility, and non-biodegradability even at a minute concentration which proves to be a significant risk to human well-being [14]. The vulnerability to Hg^{2+} ion can lead to numerous toxicological effects like brain dysfunction, DNA damage, endocrine system disorder, damage of the immune system, neurological disorder, impaired reproductive system, defective eyesight, pulmonary and cardiovascular disorders [15–18].

Considering the overwhelming toxicological effects of Fe^{3+} and Hg^{2+} ions, the urgent need to simultaneously detect even minute quantities of these heavy metals in water using the same material is of utmost importance. The best way is to detect them before their concentrations exceed the threshold limits to which they get accumulated in the environment and cause undesirable health effects. Thus, numerous assays have been devoted towards the blooming area of nanomaterials-based chemo-sensors that possess outstanding electronic, magnetic, and optical properties and can be used to detect the quantities of heavy metals in aqueous systems [19]. Various methods that can detect Fe^{3+} and Hg^{2+} ions include inductively coupled plasma mass spectrophotometry (ICPMS), colorimetry, X-ray fluorescence spectrophotometry, electrochemical methods, and atomic absorption/emission spectroscopy. These methods have excellent selectivity and sensitivity but they require trained personnel in the laboratory, involve tricky sample preparation procedures, and advanced instruments which restrict their application in Fe^{3+} and Hg^{2+} ions detection [15, 17, 20, 21]. Recently, FL sensing has attracted a lot of interest among researchers due to its tremendous benefits like outstanding sensitivity, ability to detect at minute concentration, low cost, and short response time [22]. In the last few years, CDs have emerged as a boon in the field of heavy metal ions detection as compared to metal-containing semiconductor quantum dots because they possess various advantages such as small size, biocompatibility, tunable surface functionalities, easy routes of synthesis, chemical stability, water-solubility, less toxicity, and lack of blinking [23–30]. CDs are defined as amorphous/crystalline quasi-spherical nanoparticles having a size below 10 nm containing sp^2/sp^3 nitrogen, carbon, and oxygen groups and groups generated by post-modification. The existing organic functional groups on the surface such as -COOH, $-NH_2$, -OH, and $-SO_3H$, make CDs highly soluble and stable in water and polar organic solvents. They have many applications such as photocatalysis, drug delivery, sensing, and bio-imaging. FL sensing is one of the most prominent features of CDs and it has been observed that introducing various metal ion solutions into the solution of CDs can decrease the FL intensity of CDs by aiding recombination of non-radiative holes and electrons [17, 29, 30]. There are extensive reports available on the determination of different heavy metals such as Zn, Co, Hg, Cr, Au, Ag, Fe, Pb, Co, and Cu using carbon dots [31–33]. However, for the fast monitoring of quality in complex water samples containing multiple pollutants together, simultaneous detection of multiple pollutants is preferred in comparison to single metal ion detection. Currently, CDs are becoming popular and served to be the promising FL material for the simultaneous determination of multiple ions in the same aqueous medium. For instance, CDs synthesized utilizing green *Jigua bergamot* plant as a carbon precursor were utilized for the FL sensing of Hg^{2+} and Fe^{3+} ions in the presence of HAC–NaAC and Tris–HCl buffer solutions, respectively. The LOD's for Hg^{2+} and Fe^{3+} ions were found to be 5.5 nm and 0.075 µm, respectively [34]. Fe^{3+} and Cu^{2+} were detected simultaneously with LOD's of 0.31 µm and 56 nm, respectively using hydrothermally treated nitrogen-doped carbon dots (CDs) [35]. Ren et al. utilized CDs for the determination of Hg^{2+} and Ag^{+} ions and the measured values of LOD for both the metal ions were calculated to be 4.8 nm and 1 nm, respectively [36]. Noble metal ions such as Pt^{2+}, Au^{3+}, and Pd^{2+} were also detected using red emissive carbon dots with the corresponding LOD values of 0.886 µM, 3.03 µM, and 3.29 µM, respectively [37]. Biomass-derived N, P-doped CDs have been used to determine Hg^{2+} and Cr^{6+} ions with LOD of 0.018 µM for both the metal ions [38]. Zhu et al. prepared N, S co-doped CDs for the determination of Fe^{3+} and Ag^{+} ions, and the corresponding values of LOD's were found to be 1.7 µM and 11.6 µM, respectively [39].

Herein, we report the facile synthesis of CDs through hydrothermal treatment of citric acid and ethylenediamine. The as-obtained CDs were characterized in detail by using various analytical and spectroscopic techniques such as XRD, FTIR, HRTEM and EDS. They illustrated good optical properties, hydrophilicity, photostability, strong blue fluorescence under UV light, pH stability over a range of 4–8, and ionic stability up to 0.4 M concentration of NaCl solution. Finally, they have been successfully used as a highly efficient FL sensor for the dual detection of Fe^{3+} and Hg^{2+} ions in an aqueous medium with high sensitivity and selectivity.

Experimental Section

Materials

Citric acid ($C_6H_8O_7$, 99.0%), ethylenediamine ($C_2H_8N_2$, 99%), hydrochloric acid (HCl, 37%), sodium hydroxide (NaOH, 97%), and inorganic salts such as sodium chloride (NaCl, 99%), mercury (II) sulfate ($HgSO_4$, 99%), manganese (II) acetate tetrahydrate ($C_4H_{14}MnO_8$, 99.5%), magnesium acetate tetrahydrate ($C_4H_{14}MgO_8$, > 98%) were obtained from Merck, India. Ferric sulfate hydrate [$Fe_2(SO_4)_3.H_2O$,

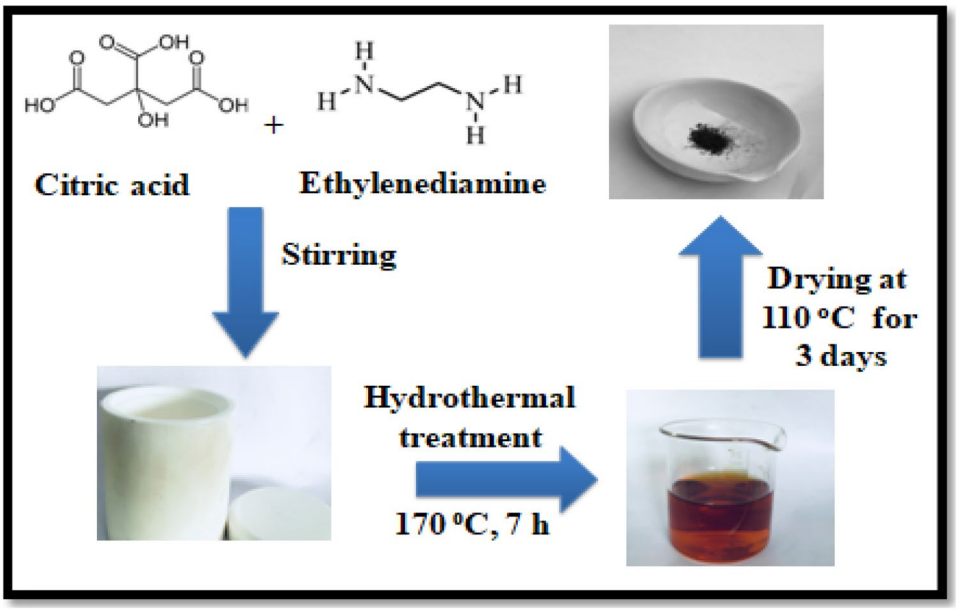

Scheme 1 Hydrothermal synthesis of CDs

75%], aluminium sulfate [$(Al_2 (SO_4)_3, > 99\%)$], and cadmium sulfate ($CdSO_4, > 97\%$) were purchased from S.D. Fine Chem. Ltd (India). Cerium nitrate hexahydrate [$Ce(NO)_3.6H_2O$, 99%)] and silver nitrate ($AgNO_3$, 99.8%) were obtained from Central Drug House Pvt. Ltd (India) and Fischer Scientific, respectively. All of the chemicals used were of analytical grade, and were utilized just as received with no further purification. Throughout the experiments, double distilled water was used as a solvent.

Synthesis of CDs

CDs were synthesized by employing a simple and easy hydrothermal approach. Typically, 0.5 g of citric acid was poured in 15 mL distilled water followed by the addition of 5 mL ethylenediamine. The as-obtained solution was allowed to stir until a clear and homogenous solution was obtained. After that, the solution was poured in a Teflon-lined stainless steel autoclave. The autoclave was kept in an oven at 170 °C for 7 h. After that, the autoclave was allowed to cool naturally at room temperature and a dark brown solution was obtained which is kept for drying at 110 °C for 3 days. Finally, CDs powder was obtained and further characterized by various techniques and have been used as a highly efficient FL sensor for the detection of heavy metal ions. Scheme 1 displayed the experimental procedure for the synthesis of CDs.

Characterizations of CDs

X-ray diffraction (XRD; PANanalyticalXpertPro.), with Cu-Kα radiation (λ = 1.54178 Å) at 45 kV and 40 mA in the 2θ ranging from 4° to 80° was used to determine the structural properties. The chemical composition of the obtained CDs was examined by using Fourier transform infrared spectroscopy (FTIR; Perkin Elmer-Spectrum RX-IFTIR) ranging from 250 to 4000 cm^{-1}. The morphology of the prepared sample was determined by a high-resolution transmission electron microscopy [HRTEM: Technai $G_2$20 (FEI) S-Twin]. UV Spectrophotometer (Systronics-2202) was used to determine the absorbance while room temperature FL analysis was performed on FL spectrophotometer (Hitachi F-7000; 5J1-004 model) having scan speed-12 nm/min, response time-0.5 s, PMT-300 V, excitation and emission slit of 10 nm, respectively. Quartz cuvette having 1 cm path length was used for FL analysis. The pH was adjusted by using a Mettler Toledo pH meter (FEP20).

Stability of CDs

The stability of CDs was investigated with respect to the ionic strength of NaCl salt, pH of the medium, and time. The impact of ionic strength on the FL intensity was investigated by using NaCl salt solutions having concentrations ranging from 0.1 M-0.4 M. To check the stability of CDs to high ionic strength, 1 mL of different concentrations of NaCl solution (0.1 M-0.4 M) was added to 1 mL stock solution (0.1 mg/mL) of CDs successively and the corresponding FL spectra were recorded. To study the impact of pH on the FL behavior of CDs, the pH of the stock solution of CDs was adjusted to different pH in the range of 2–12 by using 0.1 M aqueous solutions of HCl and 0.1 M NaOH, respectively. Then, the corresponding FL spectra of different pH solutions were recorded. To check the photostability,

the FL intensity of the stock solution of CDs was compared after a month.

FL Detection of Fe^{3+} and Hg^{2+} Ions

In this experiment, 1 mL of stock solution of CDs was transferred to a quartz cuvette and then different concentrations of 10^{-4} M solution of both the metal ions (in the range of μL) were added in a stepwise manner into the cuvette. The obtained solutions were incubated for nearly 30 s and their corresponding FL spectra were recorded at an excitation wavelength of 370 nm and PMT voltage of 300 V.

Impact of Other Interfering Ions on the FL Intensity of CDs

To determine the selectivity of the as-prepared CDs in detecting Fe^{3+} and Hg^{2+} ions, the effect of other interfering metal ions on the FL sensing of Fe^{3+} and Hg^{2+} ions was also investigated. The stock solutions of different metal ions like Na^{+}, Mn^{2+}, Ag^{+}, Ce^{3+}, Al^{3+}, Cd^{2+}, Hg^{2+}, and Mg^{2+} were prepared in distilled water (each having concentration of 10^{-2} M). The obtained solutions of metal ions were then mixed with a stock solution of CDs and allowed to stand for an incubation time of 30 s. Finally, the FL spectra of the resulting solutions were recorded at an excitation and emission slit of 10 nm, PMT voltage of 300 V, and an excitation wavelength of 370 nm.

Results and Discussion

Structural and Morphological Properties of CDs

Figure 1a displayed the HRTEM image of CDs, the typical dark spots indicated the generation of confined carbon atom clusters [40]. It was observed that CDs were spherical and very well dispersed with a size in the range of nanometers. Moreover, the absence of lattice fringes in the figure indicated that the prepared CDs were amorphous which was consistent with the previously reported literature [27, 40]. Also, the existence of diffused rings that were deprived of

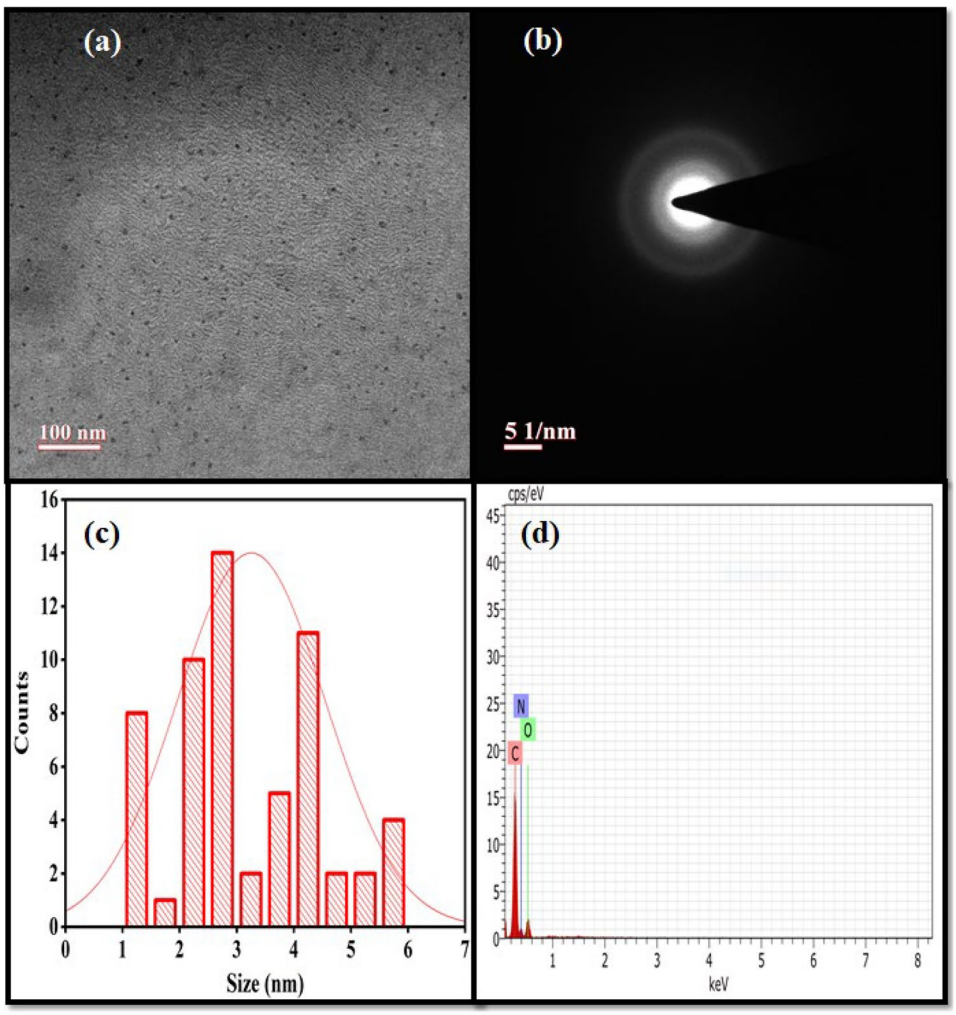

Fig. 1 Typical (**a**) HRTEM image and (**b**) SAED pattern of the as-synthesized CDs, (**c**) Size distribution histogram with average diameter, and (**d**) EDS of the as-synthesized CDs

Table 1 Percentage distribution of elements in CDs

Elements	Atomic No.	Series	Unn C [wt%]	C. Atom [wt%]
Carbon	6	K series	55.66	60.94
Oxygen	8	K series	21.88	17.98
Nitrogen	7	K series	22.45	21.08

any spots in the SAED pattern (Fig. 1b) indicates the amorphous structure of CDs [40]. From the size distribution histogram Fig. 1c, the diameter range of the CDs was found to be 1–6 nm with an average size of 2.7 nm. The distribution of elements in the sample was determined through EDS as shown in Fig. 1d. The surface composition of CDs is shown in Table 1. The CDs contained majorly carbon, oxygen, and nitrogen, with no additional impurities.

The XRD pattern of the as-prepared CDs is shown in Fig. 2a. The characteristic peak of the prepared CDs was centered at $2\theta = 23°$ corresponding to the (002) plane of graphite carbon which indicated the amorphous nature of CDs with the disordered arrangement of carbon atoms in the structure. The resulting diffraction peak was found to be consistent with the previously reported literature [27, 41, 42]. The presence of various functional groups was examined by FT-IR as shown in Fig. 2b. In FT-IR analysis of CDs, a wide absorption band at 3296 cm^{-1} was attributed to the O–H and -NH_2 functional groups. While a small absorption band at 2940 cm^{-1} was assigned to the C-H stretching vibration [27]. The absorption band at 1564 cm^{-1} was ascribed to the N–H bending and C-N stretching vibration while the absorption bands at 1292 $cm^{-1}$and 1118 cm^{-1} were assigned to the C-O stretching vibrations [43–46].The absorption bands at 1439 cm^{-1} and around 600–895 cm^{-1} were attributed to the out of plane bending vibrations of aromatic C-H [43, 47, 48]. And, a sharp absorption band at 1655 cm^{-1} indicated the existence of amide linkage (-CONH) in CDs which implied that -NH_2 groups were present on the surface of CDs [45]. The results of FTIR analysis indicated that the surface of CDs consisted of hydroxyl, carboxylic, and amide groups.

Optical Properties of Prepared CDs

The optical properties of CDs were examined using FL spectroscopy and UV–vis spectroscopy. The FL spectra of CDs is illustrated in Fig. 3a. It was found that there is no effect on the peak position of the emitted wavelength (457 nm) when the excitation wavelength varied from 330 to 390 nm. This implied the excitation independent FL behavior of CDs which confirms that CDs possess the homogeneous structure [49]. The maximum FL intensity was observed when an excitation wavelength of 370 nm was used and this wavelength was chosen as the excitation wavelength for further experimental procedures. Under UV light irradiation (18 W Philips tube with wavelength of 365 nm), a strong blue FL was observed from CDs solution while under daylight the solution was colorless (Fig. 3b). The results of absorption spectra of CDs are shown in Fig. 3b. The as-prepared CDs displayed an intense absorbance peak at around 243 nm and a broad peak was observed at 348 nm. The peak at 243 nm might be due to the л-л* transition of C = C bonds while the shoulder peak at 348 nm might be due to the n-л*transitions of C = O bonds [41, 50].

Stability of CDs

The effect of pH is shown in Fig. 3c which indicates that the FL intensity was low for $pH < 3$, this might be due to the protonation of ammonium salt (-NH_3^+) and carboxyl groups (-COOH) which may result in the formation of aggregates of CDs and thus leading to the decreased FL intensity [28]. No obvious change in the FL intensity has been noted in the pH range of 4–8 due to the saturation of the protonation of N sites on the surface of CDs [51]. Also, a decreased FL intensity was observed in the pH range of 8–12. This is because, at higher values of pH, deprotonation of -COOH and -OH groups occurs due to which the surface of CDs will become negative resulting in the decreased FL intensity [52]. Therefore, the FL intensity of CDs can get influenced under highly

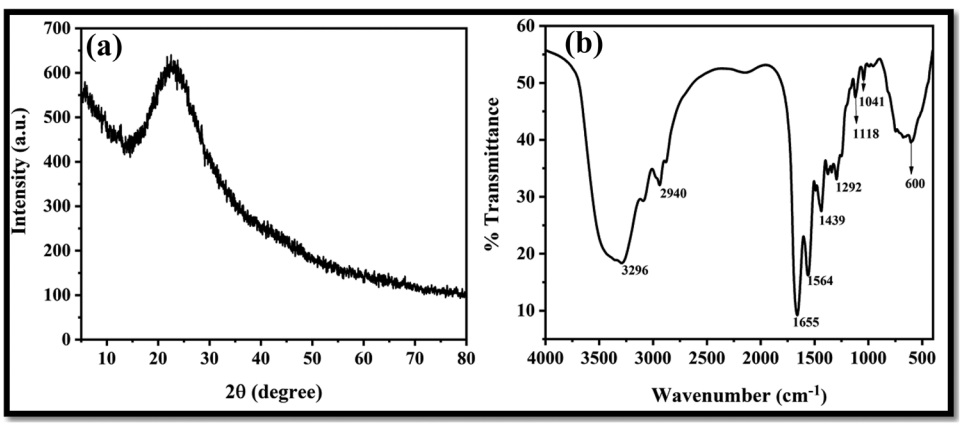

Fig. 2 (**a**) XRD pattern and (**b**) FTIR spectrum of the as-prepared CDs

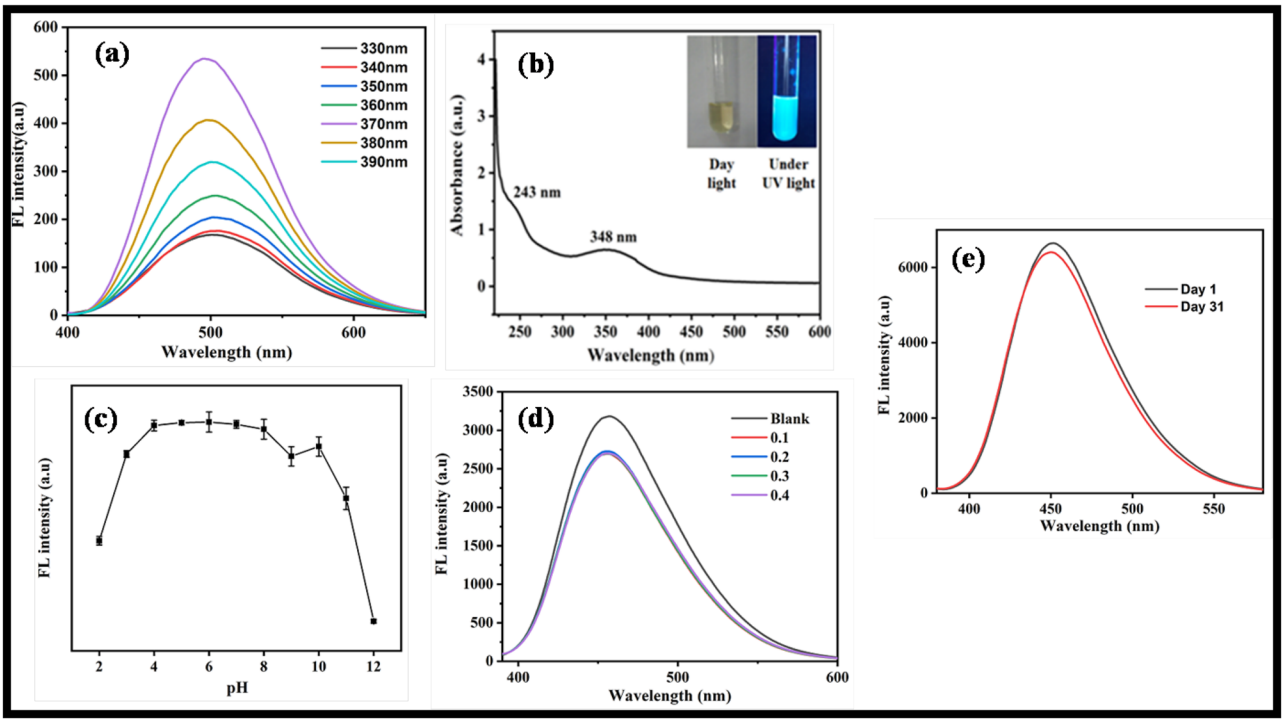

Fig. 3 Typical (**a**) FL of CDs at different excitation wavelengths at room temperature (**b**) UV–vis absorption spectra of CDs, Inset (**b**) displays the picture of FL of CDs under UV and daylight illumination, Effect of (**c**) pH and (**d**) ionic strength on the FL intensity of CDs, (**e**) Photostability curve of CDs

acidic and basic pH environments. Figure 3d displayed the impact of ionic strength on the FL intensity of CDs. Interestingly, a negligible effect was observed which signifies that the as-prepared CDs have a high tolerance to solutions having high ionic strength. Also, CDs have shown excellent photostability with negligible change in the FL intensity in aqueous medium as shown in Fig. 3e.

Selectivity Towards the Detection of Fe^{3+} and Hg^{2+} Ions

To check the selectivity of CDs for Fe^{3+} and Hg^{2+} detection, the change in the value of F_0/F after adding solutions of different metal ions (Fe^{3+}, Na^{+}, Ag^{+}, Mn^{2+}, Ce^{3+}, Cd^{2+}, Al^{3+}, Hg^{2+}, and Mg^{2+}) to the stock solution of CDs were examined. It was observed that only Fe^{3+} and Hg^{2+} ions showed significant FL quenching while other interfering metal ions showed no significant FL quenching which implied that the CDs prepared in this study can serve as an efficient FL sensor for the dual-sensing of Fe^{3+} and Hg^{2+} ions as displayed in Fig. 4a. Furthermore, to check the sensitivity of the FL probe towards the determination of Fe^{3+} and Hg^{2+} ions, the FL spectra of CDs in the presence of both the ions were recorded by varying their concentrations from 10^{-1} M to 10^{-6} M (Fig. 4b, c). It was found that when the concentration of both the ions was increased from 10^{-6} M to 10^{-1} M, the FL intensity of CDs decreases gradually. The decreased FL intensity of Fe^{3+} and Hg^{2+} ions might be due to the binding of these ions with the surface functional groups (hydroxyl and amine groups) of CDs causing a non-radiative transfer of an electron from the excited state of CDs to the empty d-orbital of Fe^{3+} and Hg^{2+} ions. Thus resulting in a quenched FL intensity [53–56].

FL Detection of Fe^{3+} and Hg^{2+} Ions

The abundant hydroxyl, carboxyl, and amino groups have a great affinity towards these metal ions in an aqueous medium. It was found that the FL intensity decreased rapidly after adding Fe^{3+} and Hg^{2+} ions to the stock solution of CDs as shown in Fig. 5a, c and the corresponding linearly fitted calibration curves were displayed in Fig. 5b, d which were obtained by using Stern–Volmer equation given below:

$$\frac{F_o}{F} = 1 + K_{SV}[Q]$$

where 'F_0' is the FL intensity of the aqueous solution of CDs and 'F' is the FL intensity of CDs after the addition of Fe^{3+} and Hg^{2+} ions, respectively. [Q] is the concentration of quencher, i.e. Fe^{3+} and Hg^{2+} ions and K_{SV} is the Stern Volmer constant. A good linearity was obtained between

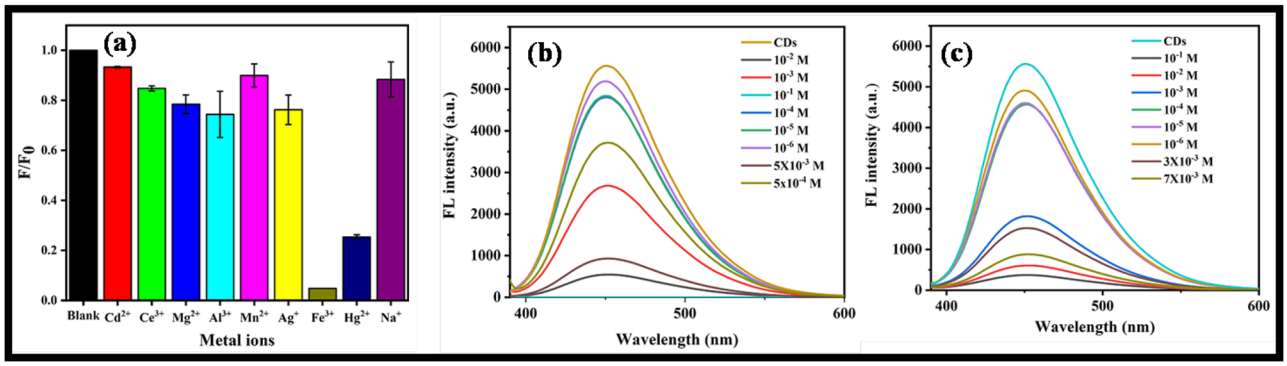

Fig. 4 (**a**) Selective FL quenching of Fe^{3+} and Hg^{2+} ions, FL spectra of the as-synthesized CDs in the presence of different amounts (10^{-1} M-10^{-6} M) of (**b**) Fe^{3+} ions and (**c**) Hg^{2+} ions

F_0/F and the concentration of Fe^{3+} and Hg^{2+} ions over the concentration range of 0–50 µM, respectively as displayed in Fig. 5b, d. The LOD (3 σ/K, where 'σ' is the standard deviation and 'K' is the slope of Stern–Volmer plot) for Fe^{3+} and Hg^{2+} ions were found to be 0.406 µM and 0.934 µM and the corresponding values of K_{SV} were estimated to be 2.17×10^4 M^{-1} and 0.98×10^4 M^{-1}, respectively. The calculated value of LOD for Fe^{3+} ions in this work was found to be lesser than some previously reported results as given in Table 2. However, the LOD of Hg^{2+} ions was not better than other reported FL sensors because the prepared CDs were more sensitive to Fe^{3+} ions as compared to Hg^{2+} ions.

Quenching Mechanism of Fe^{3+} and Hg^{2+} Ions

Generally, the fluorescence quenching mechanisms of carbon dots consist of inner filter effect (IFE), Forster resonance energy transfer (FRET), static and dynamic quenching. IFE occurs when the absorption spectra of the quencher overlaps

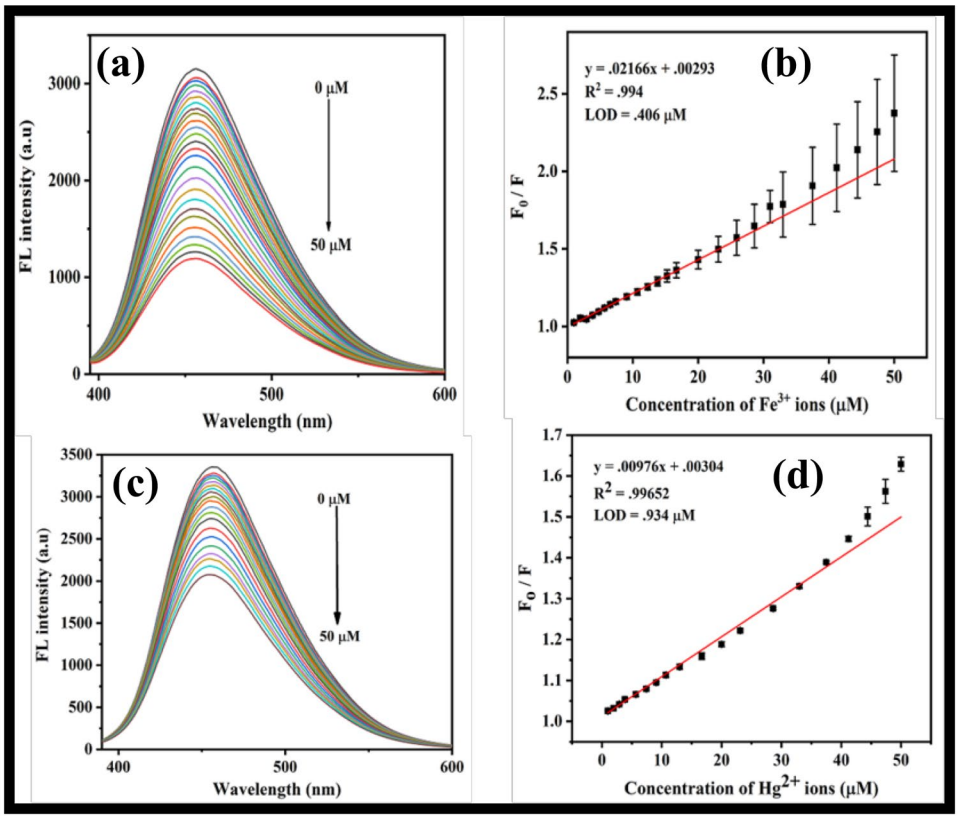

Fig. 5 (**a**) FL spectra of CDs on the addition of micro concentrations of Fe^{3+} ions (**b**) The corresponding linear fitted calibration curve of ratio of FL intensity v/s micro concentrations of Fe^{3+} ions, (**c**) FL spectra of CDs on the addition of micro concentrations of Hg^{2+} ions, (**d**) The corresponding linear fitted calibration curve of ratio of FL intensity v/s micro concentrations of Hg^{2+} ions

Table 2 List of CDs-based FL sensors for the detection of Fe^{3+} ions

Sr. No.	Precursors	Synthesis method	Linear range	LOD	Reference
1	Graphite electrode, ethanol and water	Elecrochemical	10–200 µM	1.8 µM	[57]
2	Citric acid and Tris	Hydrothermal	0-50 µM	1.3 µM	[58]
3	α-lipoic acid, sodium hydroxide and ethylenediamine	Hydrothermal	0–500 µM	4 µM	[59]
4	L-glutamate	Hydrothermal	0–50 µM	4.67 µM	[60]
5	Diammonium hydrogen citrate and urea	Hydrothermal	25–300 µM	19 µM	[61]
6	Dopamine and ethylenediamine	Hydrothermal	50–300 µM	10.8 µM	[62]
7	Alginic acid, ethanediamine	Hydrothermal	0–0.5 mM	10.98 µM	[63]
8	Citric acid and ethylenediamine	Hydrothermal	1600–6000 µM	2.37 µM	[64]
9	Citric acid and phenylalanine	Hydrothermal	0–50 µM	3.5 µM	[65]
10	Citric acid and ethylenediamine	Hydrothermal	0–50 µM	0.406 µM	This study

with the emission or excitation spectrum of CDs while in FRET, the absorption spectrum of the quencher should overlap with the emission spectrum of CDs [66].The static quenching mechanism involves the interactions between the ground state of FL material and the quencher while the dynamic quenching involves the interaction between the excited state of FL materials and the quencher [67, 68]. The quenching process is temperature dependent, in dynamic quenching, the value of K_{SV} increases with increasing temperature due to the increased number of collisions between the quencher and the excited state of the fluorophore [69, 70]. While in static quenching the value of K_{SV} decreases with increasing temperature due to the formation of the non-fluorescent complex between the quencher and the FL material which will facilitate the destruction of non-radiative e^-/h^+ recombination through a charge transfer process [71, 72].

To get a better insight of the contribution of each type of FL quenching mechanism, the absorption/excitation/emission of CDs and UV–vis absorption spectra of the quenchers were investigated. Figure 6 illustrated the absorption spectrum of Fe^{3+} and Hg^{2+} ions and the absorption, excitation and emission spectrum of CDs. Clearly, the absorption spectrum of both the ions did not overlap with neither excitation nor the emission spectrum of CDs suggesting the exclusion of IFE and FRET mechanism. To further investigate the involvement of static and dynamic quenching, the effect of temperature on the FL of CDs were examined. A good linearity in the Stern–Volmer plots of both Fe^{3+} and Hg^{2+} ions over the concentration range of

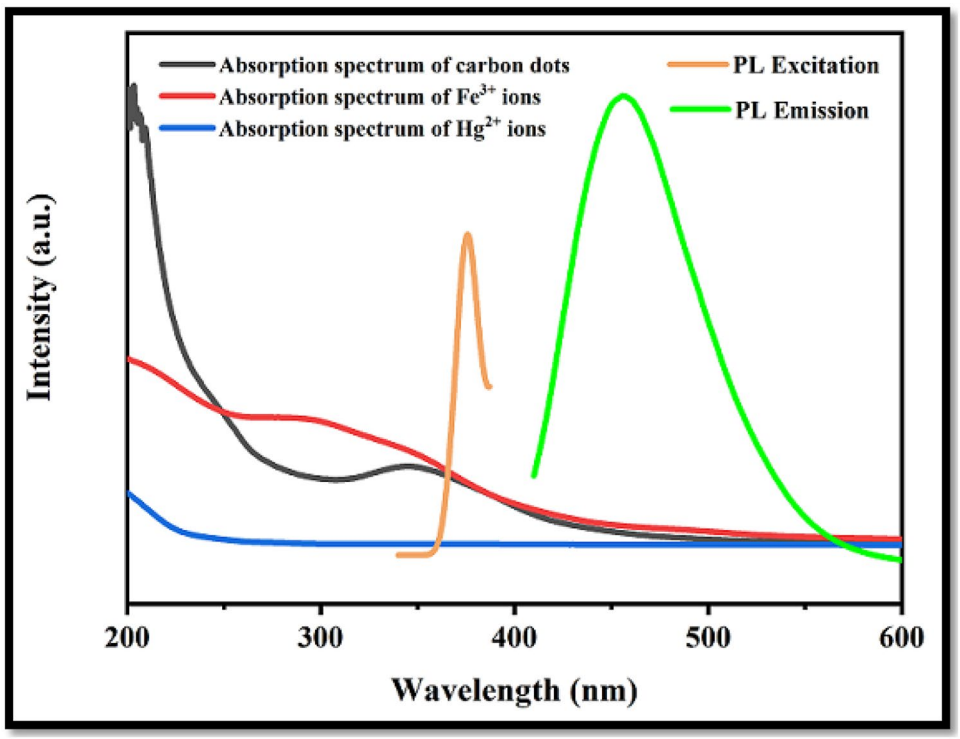

Fig. 6 Absorption spectrum of CDs, Fe^{3+} and Hg^{2+} ions and excitation/emission spectrum of CDs

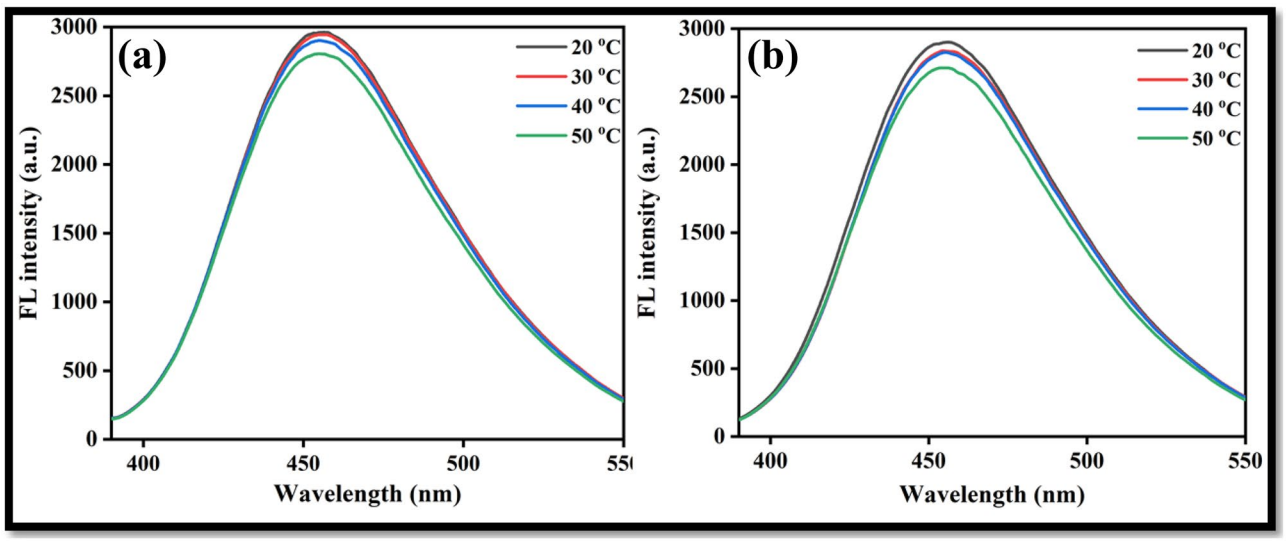

Fig. 7 Effect of temperature on the FL intensity of (**a**) Fe^{3+} treated CDs and (**b**) Hg^{2+} treated CDs

0–50 µM indicated the presence of either single static quenching or single dynamic quenching mechanism (Fig. 5). To distinguish between the static and dynamic quenching, temperature studies have been performed at temperatures of 20 °C, 30 °C, 40 °C, and 50 °C for both CDs-Fe^{3+} (Fig. 7a) and CDs-Hg^{2+} (Fig. 7b) systems. It was observed that on increasing temperature from 20 °C to 50 °C, the FL intensity decreases for both the systems which implied the existence of static quenching. The decreased FL intensity with increasing temperature was due to the dissociation of Fe^{3+}-CDs and Hg^{2+}-CDs bonds caused by the decreased binding interactions between CDs and metal ions. This will lead to the generation of the undissolved and non-fluorescent complex in the solution which will give rise to a decreased FL intensity [67, 73]. Thus, the above studies showed that static quenching mechanism was involved in the detection of Fe^{3+} and Hg^{2+} ions using CDs.

Conclusions

A facile and simple hydrothermal method was employed to synthesize hydrophilic CDs using citric acid and ethylenediamine as the precursors. The as-prepared CDs are well-dispersed, spherical, and amorphous as confirmed by results of XRD and HRTEM images. The diameter of CDs displayed a wide range (1–6 nm) with an average size of 2.7 nm. They displayed excellent optical properties such as photostability, ionic stability towards NaCl concentrations, and pH stability in the range of 4–8. Also, they exhibited excitation independent and concentration-dependent PL behavior in the visible region. The as-prepared CDs have been used successfully as a highly efficient 'turn-off' fluorescent probe for the simultaneous detection of Fe^{3+} and Hg^{2+} ions in an aqueous medium with good sensitivity and selectivity through a principle of static quenching mechanism. The estimated values of LOD's for Fe^{3+} and Hg^{2+} ions were found to be 0.406 µM and 0.934 µM, respectively. A good linearity was obtained between the concentration of both metal ions and the quenching rate over a concentration range of 0–50 µM. We conclude that the as-prepared environment-friendly CDs can serve as a potential FL sensor for monitoring the quality of water samples containing both Fe^{3+} and Hg^{2+} ions simultaneously. The present work provides an effective strategy for the development of more advanced FL sensors that can be used to detect multiple heavy metal ions simultaneously in complex water samples.

Acknowledgements The present work is supported by TEQIP-III grant of Dr. S.S.B University Institute of Chemical Engineering and Technology, Panjab University, Chandigarh. The authors are also grateful to SAIF department, Panjab University, Chandigarh and Malviya National Institute of Technology Jaipur for providing the instrumental facilities for the characterization of the prepared samples.

Author's Contributions **Shafali**: Conceptualization, Methodology, Data curation, Writing—original draft. **Sushil Kumar Kansal**: Conceptualization, Resources, Writing—original draft and Supervision.

Funding The present work is supported by TEQIP-III grant of Dr. S.S.B University Institute of Chemical Engineering and Technology, Panjab University, Chandigarh.

Data Availability The datasets used and analyzed during the current study are available from the corresponding author on reasonable request.

Declarations

Ethical Approval Not applicable.

Consent to Participate Informed consent was obtained from all individual participants included in the study.

Consent to Publish The participant has consented to the submission of the case report to the journal.

Conflicts of Interest There are no conflicts of interest to declare.

References

1. Vardhan KH, Kumar PS, Panda RC (2019) A review on heavy metal pollution, toxicity and remedial measures: current trends and future perspectives. J Mol Liquids 290:111197
2. World Health Organization (2015) Progress on sanitation and drinking water. Update and MDG Assessment. https://www.unicef.org/publications/index_82419.html
3. Hallberg GR (1987) The impacts of agricultural chemicals on ground water quality. GeoJournal 15:283–295
4. Stazi V, Tomei MC (2018) Enhancing anaerobic treatment of domestic wastewater: state of the art, innovative technologies and future perspectives. Sci Total Environ 635:78–91
5. Hairom NHH, Soon CF, Mohamed RMSR, Morsin M, Zainal N, Nayan N, Zulkifli CZ, Harun NH (2021) A review of nanotechnological applications to detect and control surface water pollution. Environ Technol Innov 24:102032
6. Shah ZU, Parveen S (2021) Pesticides pollution and risk assessment of river Ganga: A review. Heliyon 7:e07726
7. Zamora-Ledezma C, Negrete-Bolagay D, Figueroa F, Zamora-Ledezma E, Ni M, Alexis F, Guerrero VH (2021) Heavy metal water pollution: a fresh look about hazards, novel and conventional remediation method. Environ Technol Innov 22:101504
8. Naidu R, Biswas B, Willet IR, Cribb J, Singh BK, Nathanail CP, Cuolon F, Semple KT, Jones KC, Barclay A, Aitken RJ (2021) Chemical pollution: a growing peril and potential catastrophic risk to humanity. Environ Int 156:106616
9. Zhou Q, Yang N, Li Y, Ren B, Ding X, Bian H, Yao X (2020) Total concentrations and sources of heavy metal pollution in global river and lake water bodies from 1972 to 2017. Glob Ecol Conserv 22:e00925
10. Wongsasuluk P, Chotpantarat S, Siriwong W, Robson M (2014) Heavy metal contamination and human health risk assessment in drinking water from shallow groundwater wells in an agricultural area in Ubon Ratchathani province, Thailand. Environ Geochem Health 36:169–182
11. Song P, Zhang L, Long H, Meng M, Liu T, Yin Y, Xi R (2017) A multianalyte fluorescent carbon dots sensing system constructed based on specific recognition of Fe (III) ions. RSC Adv 7:28637–28646
12. Chandra S, Mahtoa TK, Chowdhuria AR, Das B, Sahua SK (2017) One step synthesis of functionalized carbon dots for the ultrasensitive detection of *Escherichia coli* and iron (III). Sens Actuators, B Chem 245:835–844
13. Khan ZMSH, Rahman RS, Shumaila IS, Zulfequar M (2019) Hydrothermal treatment of red lentils for the synthesis of fluorescent carbon quantum dots and its application for sensing Fe^{3+}. Opt Mater 91:386–395
14. Zhang R, Chen W (2014) Nitrogen-doped carbon quantum dots: Facile synthesis and application as a turn-off fluorescent probe for detection of Hg^{2+} ions. Biosens Bioelectron 55:83–90
15. Cai L, Fu Z, Cui F (2020) Synthesis of carbon dots and their application as turn off-on fluorescent sensor for mercury (II) and glutathione. J Fluoresc 30:11–20
16. Rice KM, Walker EM, Wu M, Gillette C, Blough ER (2014) Environmental mercury and its toxic effects. J Prev Med Public Health 47:74–83
17. Li Y, Zhang ZY, Yang HF, Shao G, Gan F (2018) Highly selective fluorescent carbon dots probe for mercury (II) based on thymine-mercury (II)-thymine structure. RSC Adv 8:3982
18. Ren G, Meng Y, Zhang Q, Tang M, Zhu B, Chai F, Wang C, Su Z (2018) Nitrogen-doped carbon dots for the detection of mercury ions in living cells and visualization of latent fingerprints. New J Chem 42:6824
19. Zhou L, Lin Y, Huang Z, Ren J, Qu X (2012) Carbon nanodots as fluorescence probes for rapid, sensitive, and label-free detection of Hg^{2+} and biothiols in complex matrices. Chem Commun 48:1147–1149
20. Lan M, Zhao S, Wei X, Zhang K, Zhang Z, Wu S, Wang P, Zhang W (2019) Pyrene-derivatized highly fluorescent carbon dots for the sensitive and selective determination of ferric ions and dopamine. Dyes Pigm 170:107574
21. Lv P, Yao Y, Zhou H, Zhang J, Pang Z, Ao K, Cai Y, Wei Q (2017) Synthesis of novel nitrogen-doped carbon dots for highly selective detection of iron ion. Nanotechnology 28:165502
22. Sun X, Lei Y (2017) Fluorescent carbon dots and their sensing applications. TrAC, Trends Anal Chem 89:163–180
23. Li X, Zheng Y, Tang Y, Chen Q, Gao J, Luo Q, Wang Q (2019) Efficient and visual monitoring of cerium (III) ions by green-fluorescent carbon dots and paper-based sensing. Spectrochim Acta Part A Mol Biomol Spectrosc 206:240–245
24. Murugan N, Prakash M, Jayakumar M, Sundaramurthy A, Sundramoorthy AK (2019) Green synthesis of fluorescent carbon quantum dots from *Eleusinecoracana* and their application as a fluorescence turn-off sensor probe for selective detection of Cu^{2+}. Appl Surf Sci 476:468–480
25. Bano D, Kumar V, Chandra S, Singh VK, Mohan S, Singh DK, Talat M, Hasan SH (2019) Synthesis of highly fluorescent nitrogen-rich carbon quantum dots and their application for the turn-off detection of cobalt (II). Opt Mater 92:311–318
26. Tabaraki R, Sadeghinejad N (2018) Microwave-assisted synthesis of doped carbon dots and their application as green and simple turn off–on fluorescent sensor for mercury (II) and iodide in environmental samples. Ecotoxicol Environ Saf 153:101–106
27. Sharma S, Umar A, Mehta SK, Kansal SK (2017) Fluorescent spongy carbon nanoglobules derived from pineapple juice: A potential sensing probe for specific and selective detection of chromium (VI) ions. Ceram Int 43:7011–7019
28. Wang R, Wang X, Sun Y (2017) One-step synthesis of self-doped carbon dots with highly photoluminescence as multifunctional biosensors for detection of iron ions and pH. Sens Actuators B Chem 241:73–79
29. Sharma S, Umar A, Sood S, Mehta SK, Kansal SK (2018) Photoluminescent C-dots: An overview on the recent development in the synthesis, physiochemical properties and potential applications. J Alloy Compd 748:818–853
30. Huang S, Li W, Han P, Zhou X, Cheng J, Wen H, Xue W (2019) Carbon quantum dots: synthesis, properties, and sensing applications as a potential clinical analytical method. Anal Methods 11:2240–2258
31. Zou L, Gu Z, Sun M (2015) Review of the application of quantum dots in the heavy-metal detection. Toxicol Environ Chem 97:477–490
32. Devi P, Rajput P, Thakur A, Kim KH, Kumar P (2019) Recent advances in carbon quantum dot-based sensing of heavy metals in water. TrAC Trends Anal Chem 114:171–195
33. Gao X, Du C, Zhuang Z, Chen WJ (2016) Carbon quantum dot-based nanoprobes for metal ion detection. J Matet Chem C 4:6927–6945

34. Yu J, Song N, Zhang YK, Zhong SX, Wang AJ, Chen J (2015) Green preparation of carbon dots by *Jinhua bergamot* for sensitive and selective fluorescent detection of Hg^{2+} and Fe^{3+}. Sens Actuators B Chem 214:29–35
35. Bandi R, Dadigala R, Gangapuram BR, Sabir FK, Alle M, Lee SH, Guttena V (2020) N-Doped carbon dots with pH-sensitive emission, and their application to simultaneous fluorometric determination of iron (III) and copper (II). Microchim Acta 187:30. https://doi.org/10.1007/s00604-019-4017-1
36. Ren G, Zhang Q, Li S, Fu S, Chai F, Wang C, Qu F (2017) One pot synthesis of highly fluorescent N doped C-dots and used as fluorescent probe detection for Hg^{2+} and Ag^{+} in aqueous solution. Sens Actuators B Chem 243:244–253
37. Gao W, Song H, Wang X, Liu X, Pang X, Zhou Y, Gao B, Peng X (2018) Carbon dots with red emission for sensing of Pt^{2+}, Au^{3+}, and Pd^{2+} and their bio applications in vitro and in vivo. ACS Appl Mater Interfaces 10:1147–1154
38. Singh AK, Singh VK, Singh M, Singh P, Khadim SR, Singh U, Koch B, Hasan SH, Asthana RK (2019) One pot hydrothermal synthesis of fluorescent NP-carbon dots derived from *Dunaliella salina* biomass and its application in on-off sensing of Hg (II), Cr (VI) and live cell imaging. J Photochem Photobiol A 376:63–72
39. Zhu X, Wang J, Zhu Y, Jiang H, Tan D, Xu Z, Mei T, Li J, Xue L, Wang X (2018) Green emitting N, S-co-doped carbon dots for sensitive fluorometric determination of Fe (III) and Ag (I) ions, and as a solvatochromic probe. Microchim Acta 185:510. https://doi.org/10.1007/s00604-018-3045-6
40. Siddique AB, Pramanick AK, Chatterjee S, Ray M (2018) Amorphous carbon dots and their remarkable ability to detect 2,4,6-trinitrophenol. Sci Rep 8:9770. https://doi.org/10.1038/s41598-018-28021-9
41. Liu Y, Zhou L, Li Y, Deng R, Zhang H (2016) Facile synthesis of nitrogen-doped carbon dots with robust fluorescence in a strongly alkaline solution and a reversible fluorescence 'off-on' switch between strongly acidic and alkaline solutions. RSC Adv 6:108203–108208
42. Liu SS, Wang CF, Li CX, Wang J, Mao LH, Chen S (2014) Hair-derived carbon dots toward versatile multidimensional fluorescent materials. J Mater Chemistry C 2:6477–6483
43. Zulfajri M, Gedda G, Chang CJ, Chang YP, Huang GG (2019) Cranberry beans derived carbon dots as a potential fluorescence sensor for selective detection of fe^{3+} ions in aqueous solution. ACS Omega 4:15382–15392
44. Zheng M, Xie Z, Qu D, Li D, Du P, Jing X, Sun Z (2013) On-off-on fluorescent carbon dot nanosensor for recognition of chromium (vi) and ascorbic acid based on the inner filter effect. ACS Appl Mater Interfaces 5:13242–13247
45. Du F, Zeng F, Ming Y, Wu S (2013) Carbon dots-based fluorescent probes for sensitive and selective detection of iodide. Microchim Acta 180:453–460
46. Mutuyimana FP, Liu J, Nsanzamahoro S, Na M, Chen H, Chen X (2019) Yellow-emissive carbon dots as a fluorescent probe for chromium(VI). Microchim Acta 186:163. https://doi.org/10.1007/s00604-019-3284-1
47. Joseph J, Anappara AA (2017) Ellagic acid-functionalized fluorescent carbon dots for ultrasensitive and selective detection of mercuric ions via quenching. J Lumin 192:761–766
48. Chimeno-Trinchet C, Pacheco ME, Fernandez-Gonzalez A, Diaz-Garcia ME, Badia-Laino R (2020) New metal-free nanolubricants based on carbon-dots with outstanding antiwear performance. J Ind Eng Chem 87:152–161
49. Rong MC, Zhang KX, Wang YR, Chen X (2017) The synthesis of B, N-carbon dots by a combustion method and the application of fluorescence detection for Cu^{2+}. Chin Chem Lett 28:1119–1124
50. Zhou Y, Liyanage PY, Geleroff DL, Peng Z, Mintz KJ, Hettiarachchi SD, Pandey RR, Chusuei CC, Blackwelder PL, Leblanc RM (2018) Photoluminescent carbon dots: a mixture of heterogeneous fractions. ChemPhysChem 19:2589
51. Qian Z, Ma J, Shan X, Feng H, Shao L, Chen J (2014) Highly luminescent N-doped carbon quantum dots as an effective multifunctional fluorescence sensing platform. Chemi Eur J 20:2254–2263
52. Wang L, Li M, Li W, Han Y, Liu Y, Li Z, Zhang B, Pan D (2018) Rationally designed efficient dual-mode colorimetric/fluorescence sensor based on carbon dots for detection of pH and Cu^{2+} ions. ACS Sustain Chem Eng 6:12668–12674
53. Gong X, Lu W, Paau MC, Hu Q, Wu X, Shuang S, Dong C, Choi MMF (2015) Facile synthesis of nitrogen-doped carbon dots for Fe^{3+} sensing and cellular imaging. Anal Chim Acta 861:74–84
54. Li W, Zhang Z, Kong B, Feng S, Wang J, Wang L, Yang J, Zhang F, Wu P, Zhao D (2013) Simple and green synthesis of nitrogen-doped photoluminescent carbonaceous nanospheres for bioimaging. Angew Chem Int Ed 52:8151–8155
55. Du Y, Guo S (2016) Chemically doped fluorescent carbon and graphene quantum dots for bioimaging, sensor, catalytic and photoelectronic applications. Nanoscale 8:2532–2543
56. Yahyazadeh E, Shemirani F (2019) Easily synthesized carbon dots for determination of mercury (II) in water samples. Heliyon 5:e01596
57. Liu M, Xu Y, Niu F, Gooding JJ, Liu J (2016) Carbon quantum dots directly generated from electrochemical oxidation of graphite electrodes in alkaline alcohols and the applications for specific ferric ion detection and cell imaging. Analyst 141:2657
58. Zhou M, Zhou Z, Gong A, Zhang Y, Li Q (2015) Synthesis of highly photoluminescent carbon dots via citric acid and Tris for iron (III) ions sensors and bioimaging. Talanta 143:107–113
59. Ding H, Wei JS, Xiong HM (2014) Nitrogen and sulfur co-doped carbon dots with strong blue luminescence. Nanoscale 6:13817–13823
60. Yu J, Xu C, Tian Z, Lin Y, Shi Z (2016) Facilely synthesized N-doped carbon quantum dots with high fluorescent yield for sensing Fe^{3+}. New J Chem 40:2083–2088
61. Khan WU, Wang D, Zhang W, Tang Z, Ma X, Ding X, Du S, Wang Y (2017) High quantum yield green-emitting carbon dots for Fe (III) detection, biocompatible fluorescent ink and cellular imaging. Sci Rep 7:14866
62. Li G, Lv N, Bi W, Zhang J, Ni J (2016) Nitrogen-doped carbon dots as a fluorescence probe suitable for sensing Fe^{3+} under acidic conditions. New J Chem 40:10213–10218
63. Liu Y, Liu Y, Park SJ, Zhang Y, Kim T, Chae S, Park M, Kim HY (2015) One-step synthesis of robust nitrogen-doped carbon dots: acid-evoked fluorescence enhancement and their application in Fe^{3+} detection. J Materi Chem A 3:17747–17754
64. Lu F, Zhou YH, Wu LH, Qian J, Cao S, Deng YF, Chen Y (2019) Highly fluorescent nitrogen-doped graphene quantum dots' synthesis and their applications as fe (iii) ions sensor. Int J Opt 2019:9. https://doi.org/10.1155/2019/8724320
65. Chahal S, Yousefi N, Tufenkji N (2020) Green synthesis of high quantum yield carbon dots from phenylalanine and citric acid: role of stoichiometry and nitrogen doping. ACS Sustain Chem Eng 8:5566–5575
66. Zu F, Yan F, Bai Z, Xu J, Wang Y, Huang Y, Zhou X (2017) The quenching of the fluorescence of carbon dots: a review on mechanisms and applications. Microchim Acta 184:1899–1914
67. Shah H, Xin Q, Jia X, Gong JR (2019) Single precursor-based luminescent nitrogen-doped carbon dots and their application for iron (III) sensing. Arab J Chem 12:1083–1091
68. Wu H, Pang LF, Fu MJ, Guo XF, Wang H (2020) Boron and nitrogen codoped carbon dots as fluorescence sensor for Fe^{3+} with improved selectivity. J Pharm Biomed Anal 180:113052
69. Deepa HR, Thipperudrappa J, Kumar HMS (2020) Effect of temperature on fluorescence quenching and emission characteristics of laser dyes. J Phys Conf Ser 1473:012046

70. Song Y, Zhu S, Xiang S, Zhao X, Zhang J, Zhang H, Fu Y, Yang B (2014) Investigation into the fluorescence quenching behaviors and applications of carbon dots. Nanoscale 6:4676–4682
71. Kaur J, Sharma S, Mehta SK, Kansal SK (2020) Highly photoluminescent and pH sensitive nitrogen doped carbon dots (NCDs) as a fluorescent sensor for the efficient detection of Cr (VI) ions in aqueous media. Spectrochim Acta Part A Mol Biomol Spectrosc 227:117572
72. Yu S, Chen K, Wang F, Zhu Y, Zhang X (2016) Polymer composite fluorescent hydrogel film based on nitrogen doped carbon dots and their application in the detection of Hg^{2+} ions. Luminescence 32:970–977
73. Issa MA, Abidin ZZ, Sobri S, Rashid SA, Mahdi MA, Ibrahim NA (2020) Fluorescent recognition of Fe^{3+} in acidic environment by enhanced-quantum yield N-doped carbon dots: optimization of variables using central composite design. Sci Rep 10:11710